J. Plasma Fusion Res. SERIES, Vol.1 (1998) 507–510

Nonlinear Drift Orbit Mappings in Helical Systems

YAMAGISHI Tomejiro
Tokyo Metropolitan Institute of Technology, Hino, Tokyo 191-0065, Japan

(Received: 30 September 1997/Accepted: 22 October 1997)

Abstract

Nonlinear behaviors of electron drift orbits are investigated by a simple mapping model in helical systems. With a small dissipation, the phase portrait of Poincare mapping change significantly as compare to that of area preserving one. Global stability of 280 × 280 orbits are graphically investigated by calculating the Lyapunov exponent for each orbit, and found that the effect of dissipations change little the global stability characteristics. The dressed winding number of orbits shows clearly the mode locking phenomenon. In the l=1 helical configuration, the 1/f-noise spectrum is observed.

Keywords:

drift orbit mapping, helical configuration, dissipation, stochastisity, Lyapunov exponent, two-dimensional graphics, 1/f-noise spectrum.

1. Introduction

The nonlinear mapping in the area preserving system has been studied completely separately from the dissipative system, because chaotic behaviors of these systems are entirely different, *i.e.*, the area preserving system may show ergodic behavior while the dissipative system may tend to a strange attractor. In numerical evaluation of orbits in the area preserving Hamiltonian system, therefore, the Jacobian of the transformation must precisely be kept unity, otherwise the system may change to a dissipative system. In actual physical systems, however in any case, we have more or less dissipations.

The purpose of this paper is to study the effect of dissipation on the drift orbit mapping in helical systems. Based on the drift approximation, the dissipation is introduced through generalized Ohm's law. Since our mapping equations are applicable to the dissipative and area preserving systems by changing the particle dissipation, we can study how orbits may change by changing from the area preserving system to the dissipative system. By performing mappings by computer, it will be shown in section 3 that for small dissipations orbit points stay in certain annular region instead of tending to a strange attractor. By evaluating the Lyapunov exponent for 280 × 280 orbits, it will be also shown that the global stability characteristics of helical configurations change little, although the phase space structure of mappings change significantly with a small dissipation.

2. Drift Orbit Model

We start with the particle guiding center velocity v_G which can be expressed by the sum:

$$v_G = v_\parallel + v_\perp \tag{1}$$

The parallel component along the magnetic field can be expressed by $v_\parallel = v_\parallel b$ with $b = B/B$. The perpendicular component $v_\perp$ may involve the E × B drift and the curvature drift components. We introduce here another perpendicular component from generalized Ohm's law in the form

$$v_D = -D_e (1 + \tau) \frac{\nabla n}{n} \tag{2}$$

where D_e is electron diffusion coefficient and $\tau = T_e/T_i$

Corresponding author's e-mail: tyamagi@cc.tmit.ac.jp

is the electron temperature to ion temperature ratio, and other notations are standard.

Since v_D is a fluid velocity, we consider v_G as an averaged velocity over the Maxwellian plasma and study the flow lines of "averaged particle (electron)" with thermal velocity v_e. We assume the parallel motion along the magnetic field lines gives the principal term and v_D as a weak perturbation.

In the cylindrical coordinate system (r, θ, z), each component of the velocity can be written in the from

$$v_r = \frac{dr}{dt} = v_{\parallel} b_r - D_e (1+\tau) \frac{n'}{n} \tag{3}$$

$$v_\theta = r\frac{d\theta}{dt} = v_{\parallel} b_\theta + v_E + v_C \tag{4}$$

$$v_z = v_{\parallel} b_z \tag{5}$$

where v_E and v_c are the E×B and curvature drift velocity components, respectively.

The curvature drift velocity v_c is replaced by the diamagnetic drift velocity when we consider from the fluid view point, because v_c is canceled out by the magnetization effect[1]. The remaining diamagnetic drift velocity has, however, no radial component and does not contribute to the dissipative term in our model.

Each component of the helical magnetic field is given by[2]

$$B_r = h_r \sin u, \tag{6}$$

$$B_\theta = B_{\theta 0} + h_\theta \cos u \tag{7}$$

$$B_z = B_0 (1 - \varepsilon_h \cos u) \tag{8}$$

where $h_r = lB_0 I'_l(kr)$, $h_\theta = lRI_l(kr)$, $\varepsilon_h = lI_l(kr)$, I_l is the modified Bessel function and $u = l\theta - kz$. Integrating Eqs. (3) and (4) for one period along the toroidal direction making use of $v_{\parallel} dt = dz$, we have the displacements

$$\Delta r = \oint b_r dz - \oint D_e (1+\tau) \frac{n' dz}{n v_{\parallel}} \tag{9}$$

$$\Delta\theta = \oint \frac{b_\theta}{r} dz + \oint (v_E + v_c) \frac{dz}{r v_{\parallel}} \tag{10}$$

where the first and second terms in Eqs.(9) and (10) represent the helical field and particle drift contributions, respectively.

Substitution of Eq.(6) into the first term of Eq.(9) may yield K sin $l\theta_n$ with $K = Rh_r/B_z$. If we assume a parabolic profile for the density: $n(x) = n_0(1-x^2)$, the second dissipative term may be approximated by $c_d x$ with $c_d = -4\pi RD_0(1+\tau)/a^2 v_e$ and D_0 being the classical diffusion coefficient at the center $x=0$. Using these approximation, from Eq.(9), we have a mapping equation for the radial coordinate:

$$x_{n+1} = (1 - c_d) x_n + K \sin l\theta_n \tag{11}$$

where $x = r/a$ with a being the helical conductor radius.

Introducing Eq.(7) into the first term in Eq.(10), we have the rotational transform, ι of magnetic field lines. We assume here the first term is much larger than the contribution from the drift motions in the second term. In this case, we have mapping equation for the poloidal angle:

$$\theta_{n+1} = \theta_n + (x_{n+1}) \tag{12}$$

where ι is assumed to be a function of x_{n+1} instead of x_n in order to satisfy the area conservation when $c_d=0$. In this case, the Jacobian of the two-dimensional transformation is given by $J = |\partial(x_{n+1}, \theta_{n+1})/\partial(x_n, \theta_n)| = 1 - c_d$.

The mapping given by Eqs. (11) and (12) may be too simple to see characteristics of a realistic toroidal-helical configuration. Even in this simplest model, we find new phenomena as we shall see. To investigate a new phenomenon, we must employ as simple model as possible, and determine what is the cause of the phenomenon. Application to realistic models including the grad-B and curvature drifts may be straightforward.

We express the rotational transform in term of the shear parameter: $\iota(x) = \iota_0(1+s\,x)$ with $s = r\,\iota'/\iota$ and ι_0 being the rotational transform at $x=0$. Near the singularity of the rotational transform ι, the two-dimensional map (11) and (12) can be transformed to the separatrix map as applied to a toroidal divertor system[3]. It can also be transformed to the standard map[4, 5], and to the one-dimensional circle map[6].

3. Mapping and Two Dimensional Graphics

Applying simple equations (11) and (12), we carried out mapping $(x_n, \theta_n) \to (x_{n+1}, \theta_{n+1})$ many times by computer. First we tested mappings for magnetic field line orbits without dissipation. A result is presented in Fig.1a for 20 orbits in the $l=1$ configuration. In high temperature plasmas in strong magnetic field, the dissipation coefficient c_d is very small. For R=120 cm, a=20 cm, T=400 eV, B=5 KG and $n=10^{13}$ cm^{-3}, we have $c_d \sim 10^{-7}$. For higher density with lower temperature plasmas in lower magnetic field, the coefficient may increase upto 10^{-5}. Furthermore, if we take into account an anomalous diffusion effect, it may be larger by two order of magnitude. We assume, therefore, the range of dissipation coefficient, $c_d \leqq 10^{-3}$. Even this small range of the dissipation effect, behavior of orbit

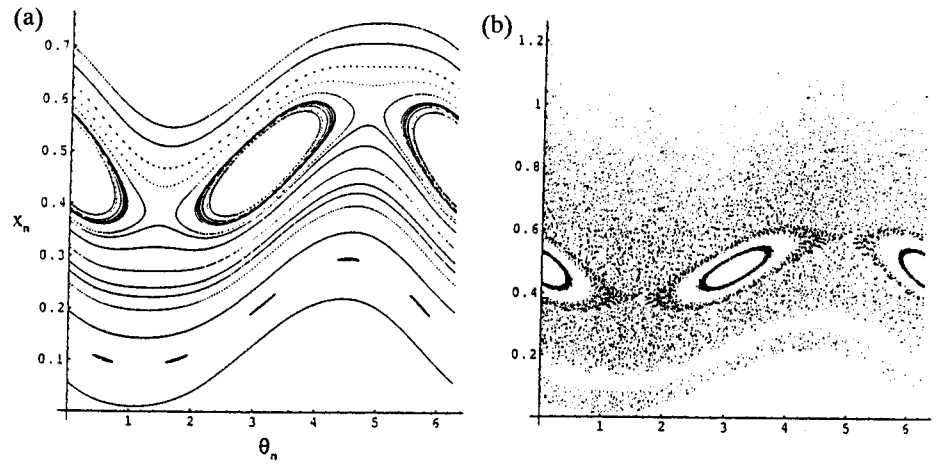

Fig. 1 Plot of 20000 (20 orbits) points mapping in helical systems with l=1, K=0.2, s=1, and ι=2.123. (a): area preserving case (c_d=0), (b): dissipative case with c_d=−0.0005.

given by mappings changes significantly. An example is shown in Fig.1(b) for the same orbits as in Fig.1(a) with c_d=−0.0005. In the dissipative case, orbits fill deformed annular region with certain thickness, which looks stochastic. This also indicates that an area preserving mappings with very small (0.05%) error in the Jacobian J changes the orbit structure from Fig.1(a) to Fig.1(b).

Whether orbits are stochastic or regular is extremely important in evaluation of plasma and thermal transport coefficients[7]. We, therefore, examined carefully the stability of such dissipative orbits by evaluating the Lyapunov exponent and also Fourier spectra. We evaluated the j-th component of the Lyapunov exponent σ_j for the two dimensional map by

$$\sigma_j = \lim_{n\to\infty} \ln |\lambda_j| \tag{13}$$

where λ_j is the eigenvalue of the n-product of the Jacobian matrix:

$$J_n = J(x_n, \theta_n)J(x_{n-1}, \theta_{n-1}) \cdots J(x_1, \theta_1). \tag{14}$$

Since the sum of Lyapunov exponents is equal to the area concentration rate A_o in the two dimensional dissipative map, $\sigma_1+\sigma_2=A_o$[5], when one component σ_1 is evaluated, the other σ_2 is given by this relation. In the area preserving map, A_o is zero and $\sigma_2=-\sigma_1$. In this case, the unstable component is $\sigma_1 \geq 0$. That is the orbit is stable only when $\sigma_1=0$ or marginally stable. When $c_d>0$ ($n'>0$), $J<1$ and the dissipative term is stabilizing, while for $c_d<0$ ($n'<0$), $J>1$ and it is destabilizing. For both cases, we use the term "dissipative". Even in the unstable case, $c_d<0$, we found that most orbits stay in certain annular region.

Since the stability of each orbit depends on many parameters such as helical amplitude K, shear parameter s, the initial position in the helical configuration and so on, in order to examine the global stability characteristics of a helical configuration, we must test the stability as many orbits as possible in the system. We evaluated the unstable component of the Lyapunov exponent σ_1 for 280 × 280 orbits with different initial positions, which are presented by a two dimensional graphics as shown in Fig.2(a) for the area preserving case.

In the two-dimensional graphics, the value of Lyapunov exponent σ_1 is shown by light and *shade, i.e.*, the dark point means that σ_1 is very close to zero or the orbit is stable, the white point means that σ_1 is largest or orbit is most unstable, and the gray point means the intermediate unstable orbit. The same two-dimensional graphics is presented for the case of dissipative case in Fig.2(b). As compared with the area preserving case in Fig.2(a), the global stability characteristics of the dissipative orbits change little, although the phase portrait of Poincare mappings in the dissipative case show significant difference as seen in Fig. 2. We can see many well behaved (black) KAM surfaces in the both cases.

In order to examine the mode locking phenomenon, we also evaluated the dressed winding number ρ defined by

$$\rho = \lim_{n\to\infty} \frac{1}{n}(\theta_n - \theta_0)$$

When we plot ρ as a function of ι, Devil's staircase appears, *i.e.*, the mode locking phenomenon is observed at the rational surfaces as in the circle map[6]. Finally we calculated the frequency power spectrum for drift orbits by the fast Fourier transform technique, and

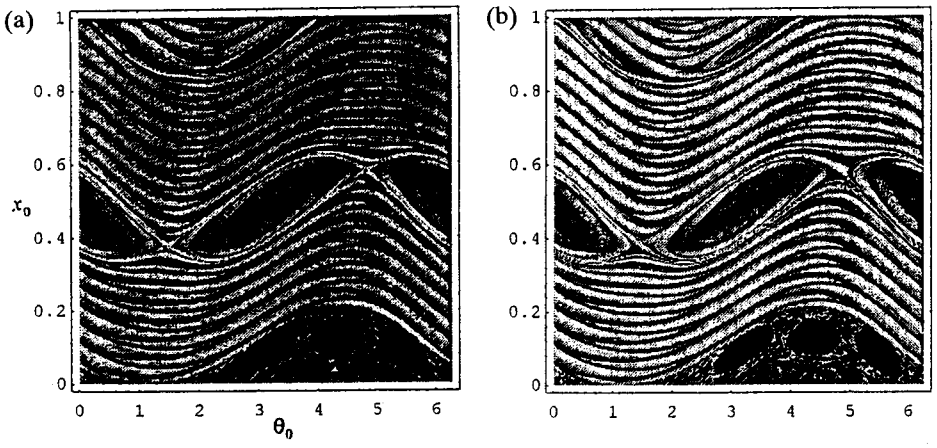

Fig. 2 Two dimensional graphicses of Lyapunov exponent for 280×280 different initial positions in helical configurations with l=1, K=0.2, ι=2.123 and s=1. (a): area preserving case (c_d=0), (b): dissipative case with c_d=−0.0005.

observed the 1/f-noise spectrum for the dissipative case in the l=1 helical configuration.

4. Conclusion

Making use of a simple mapping model based on Ohm's law, the effect of dissipation on orbit mapping is studied, and found that the orbit does not tend to a strange attractor in the small range of dissipation, $0 < c_d < 10^{-3}$. As compared with the area preserving case, however, the orbit change significantly, *i.e.*, the mapping points fill annular region with certain thickness. Most of such orbit is found to be not stochastic. The two-dimensional graphics based on the Lyapunov exponent for 280 × 280 orbits shows little difference in the global stability characteristics as compared with the area preserving case, although each mapping result is significantly different. From these results, one may conclude that the mapping method is not suitable to examine the orbit stochasticity particularly in the dissipative case.

Acknowledgment

This study is a joint research effort with the National Institute for Fusion Science.

References

[1] R.D. Hazeltine and J.D. Meiss, *Plasma Confinement*, Addidon-Wesely, New York (1992).

[2] L.S. Solovev and V.D. Shafranov, *Reviews of Plasma Physics*, Vol.5, Consultant Bureau, New York (1970).

[3] T. Yamagishi, Transactions of Fusion Technology **27**, 505 (1995).

[4] B.V. Chilikov, Physics Report **52**, 263 (1979).

[5] A.J. Lichtenberg and M.A. Lieberman, *Regular and Stochastic Motion*, Springer-Verlag, New York (1983).

[6] T. Yamagishi, Memoir of Tokyo Metropolitan Institute of Technology **10**, 208 (1996).

[7] T. Yamagishi, M.S. Chu, D.K. Bhadra and F.L. Hinton, J. Nucl. Material **128&129**, 118 (1984).